quite moisture sensitive and hydrolyzes with the preferential generation of **1** (R = $C_2H_5$).

4,8-Dichloro-4,8-diethylpyrazabole afforded access to other novel pyrazaboles. For example, it reacted with potassium methoxide in methanol at room temperature to give the first example of a *B*-alkoxypyrazabole, i.e., $(C_2H_5)(CH_3O)B(\mu\text{-pz})_2(C_2H_5)(OCH_3)$. The corresponding *B*-ethoxy derivative was obtained in similar fashion, and both were also obtained, even in much better yield, by the reaction of the chloro compound with the alcohol in the presence of triethylamine.

Both of the cited alkoxypyrazaboles were obtained as isomer mixtures, as was readily documented by the $^1H$ NMR spectra of the species. The ratio of the isomers was found to be somewhat dependent on the preparative procedure, although in each case the same one was formed in substantially larger quantity. Unfortunately, separation of the isomers has not been possible. Indeed, the existence of cis and trans isomers of pyrazaboles of the type $RR'B(\mu\text{-pz})_2BRR'$ has long been suspected,[7] but only most recently has it been documented by experiment and successful separation of conformers.[8]

4,8-Dichloro-4,8-diethylpyrazabole was also reacted with $(CF_3CO)_2O$ to give the species $R(R'O)B(\mu\text{-pz})_2BR(OR')$ with R = $C_2H_5$ and R' = $CF_3CO$ with elimination of $CF_3COCl$ and also with acetic anhydride to give the corresponding nonfluorinated species. Again, both species were obtained as mixtures of cis and trans isomers that could not be separated.

The above reactions illustrate that **1** is a valuable precursor for the synthesis of various pyrazaboles containing two different substituents at each boron atom.

**Acknowledgment.** The authors gratefully acknowledge a generous gift of *B*-triethylboroxin from Professor R. Köster, Max-Planck-Institut für Kohlenforschung, Mülheim, West Germany. This work was supported by the Office of Naval Research (K.N.) and the National Science Foundation (S.G.S.).

**Supplementary Material Available:** Listings of anisotropic thermal parameters for non-hydrogen atoms and least-squares planes for **1** with R = $C_2H_5$ (2 pages); a listing of structure factor amplitudes (22 pages). Ordering information is given on any current masthead page.

(7) Trofimenko, S. *J. Am. Chem. Soc.* **1967**, *89*, 4948-4952.

(8) Bielawski, J.; Das, M. K.; Hanecker, E.; Niedenzu, K.; Nöth, H. *Inorg. Chem.*, in press.

Contribution from the Department of Chemistry, State University of New York (SUNY) at Albany, Albany, New York 12222

# Models for Methemocyanin Derivatives: Structural and Spectroscopic Comparisons of Related Azido-Coordinated ($N_3^-$) Mono- and Dinuclear Copper(II) Complexes

Kenneth D. Karlin,* Brett I. Cohen, John C. Hayes, Amjad Farooq, and Jon Zubieta

*Received June 4, 1986*

The use of the azide ($N_3^-$) ligand as a probe of the dinuclear copper active site in the dioxygen-transport protein hemocyanin has prompted us to synthesize model complexes that may shed light on the structural and spectroscopic features associated with $N_3^-$ binding to Cu(II) in well-defined chemical systems. We report the synthesis and structural and spectroscopic properties of $N_3^-$ bound to a dinuclear Cu(II) complex and a mononuclear analogue. The dinucleating ligand, L-OH, forms a phenoxo-bridged dicopper(II) complex, **2b**, where each Cu(II) ion is also coordinated in a square-based-pyramidal geometry to the nitrogen atoms of a tridentate py2 unit (py2 = bis(2-(2-pyridyl)ethyl)amine) and to a $\mu$-1,1-$N_3^-$ ligand. A mononucleating analogue, $[Cu^{II}(L'\text{-}O^-)(N_3^-)]$ (**3b**), contains Cu(II) coordinated to the same $N_3O$ donor set provided by L'-OH and a terminally coordinated $N_3^-$ ligand in a coordination environment very similar to that found in **2b**. Compound **2b** crystallizes in the triclinic space group $P\bar{1}$ with $Z = 2$ and $a = 9.583$ (1) Å, $b = 10.123$ (2) Å, $c = 23.758$ (4) Å, $\alpha = 87.19$ (1)°, $\beta = 88.83$ (1)°, and $\gamma = 84.85$ (1)°. Complex **3b** crystallizes in the monoclinic space group $P2_1/c$, with $Z = 4$ and $a = 9.529$ (7) Å, $b = 18.950$ (2) Å, $c = 13.829$ (5) Å, and $\beta = 109.38$ (5)°. Comparisons of the charge-transfer (CT) features observed in UV-vis spectra of these complexes and related chloride and/or nitrate ion containing derivatives of L-OH, L'-OH, and py2 allow assignment of the $PhO^- \rightarrow Cu(II)$ (450-460 nm) and/or $N_3^- \rightarrow Cu(II)$ (370-405 nm) CT bands. Other structural and spectroscopic comparisons are also made.

## Introduction

Extensive spectroscopic and chemical investigations[1-4] have suggested detailed pictures of the active sites of the copper proteins hemocyanin (arthropod and mollusc dioxygen carrier) and the protein tyrosinase (monooxygenase that hydroxylates monophenols). Both of these proteins contain spectroscopically similar dinuclear copper centers that in the reduced state most likely contain three-coordinate Cu(I) with imidazole ligands.[5] Upon oxygenation, a dicopper(II) complex is formed in which two tetragonal copper(II) ions separated by 3.6 Å are thought to be bridged by an endogenous R group and the exogenous $\mu$-1,2-peroxo ligand (X) derived from dioxygen:

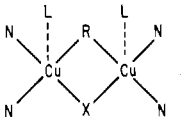


In establishment of the nature of the active site, investigations have relied heavily upon spectroscopic studies of the products of binding and interactions of small molecules such as acetate, chloride, azide, etc., in chemically modified hemocyanin or tyrosinase derivatives.[1,2,6] Details such as Cu···Cu distances in the active sites, differences among mollusc and arthropod hemocyanins, and electron delocalization in half-met ($Cu^{II}Cu^{I}$) de-

(1) (a) Solomon, E. I.; Penfield, K. W.; Wilcox, D. E. *Struct. Bonding (Berlin)* **1983**, *53*, 1-57. (b) *Copper Coordination Chemistry: Biochemical & Inorganic Perspectives*; Karlin, K. D., Zubieta, J., Eds.; Adenine: Guilderland, NY, 1983. (c) Solomon, E. I. In ref 1b, pp 1-22.

(2) Solomon, E. I. In *Copper Proteins*; Spiro, T. G., Ed.; Wiley: New York, 1981; Vol. 3, pp 41-108.

(3) (a) Co, M. S.; Hodgson, K. O.; Eccles, T. K.; Lontie, R. *J. Am. Chem. Soc.* **1981**, *103*, 984-986. (b) Co, M. S.; Hodgson, K. O. *Ibid.* **1981**, *103*, 3200-3201.

(4) Brown, J. M.; Powers, L.; Kincaid, B.; Larrabee, J. A.; Spiro, T. G. *J. Am. Chem. Soc.* **1980**, *102*, 4210-4216.

(5) Gaykema, W. P. J.; Hol, W. G. J.; Vereijken, J. M.; Soeter, N. M.; Bok, H. J.; Beintema, J. J. *Nature (London)* **1984**, *309*, 23-29.

(6) (a) Himmelwright, R. S.; Eickman, N. C.; LuBien, C. D.; Solomon, E. I. *J. Am. Chem. Soc.* **1980**, *102*, 5378. (b) Himmelwright, R. S.; Eickman, N. C.; LuBien, C. D.; Lerch, K.; Solomon, I. E. *Ibid.* **1980**, *102*, 7339. (c) Winkler, M. E.; Lerch, K.; Solomon, E. I. *Ibid.* **1981**, *103*, 7001.

0020-1669/87/1326-0147$01.50/0 

rivatives have been determined from studies on derivatives in which these ligands may act as Cu–Cu bridging groups, X.

In this regard, azide ligand binding to protein binuclear copper centers has played a key role in bioinorganic studies. This is because of the occurrence of strong charge-transfer absorptions in the visible region, accessibility by IR and EPR spectroscopic techniques, and its variable mode of binding.[7] Terminal (A),[8-10] $\mu$-1,1 bridging (B),[10-12] and $\mu$-1,3 bridging (C)[8-10,13-15] are all

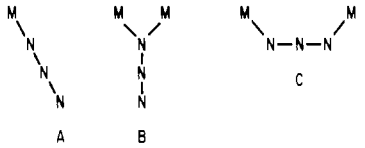

known in copper chemistry, and both modes A and C have been proposed to occur in methemocyanin derivatives.[1,2] Because of the importance of azide coordination in protein studies, we[16-18] and others[13,14,19] have sought to examine its coordination properties in relevant model systems.

In investigations aimed at modeling either reduced (deoxy)[20-25] or oxidized (oxy[21-25] or met[16-18]) dicopper protein centers, we have developed the chemistry of the dinucleating phenol-containing ligand L-OH, which forms the phenoxo-bridged complex **1**. These can be treated to form other phenoxo and X doubly bridged compounds (**2**), including $X = N_3^-$ (**2b**). Here, we report the synthesis and characterization of the $\mu$-1,1-azido-bridged dicopper(II) complex **2b**, which we had reported in an earlier communication.[16] In order to elucidate the structural and spectroscopic effects of azide coordination to either one or two Cu(II) ions in similar environments, we have also synthesized a monomeric analogue of L-OH, L'-OH. We concurrently report the synthesis and structure of $[Cu(L'\text{-}O^-)(N_3)]\cdot H_2O$ (**3b**). Chloride ($X = Cl^-$) containing derivatives **2a** and **3a**, and complexes containing only the $N_3$ tridentate bis(2-(2-pyridyl)ethyl)amine (py2) (**4a,b**), i.e. without phenoxo coordination, have also been examined in order to help sort out and assign the electronic spectral transitions in these complexes.

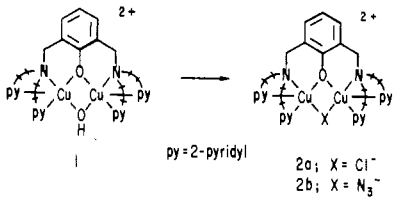

py = 2-pyridyl

2a; X = $Cl^-$
2b; X = $N_3^-$

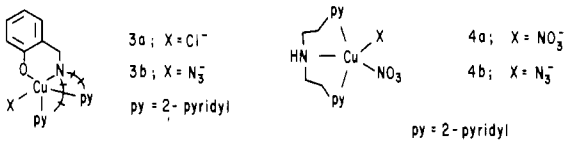

3a; X = $Cl^-$
3b; X = $N_3^-$
py = 2-pyridyl

4a; X = $NO_3^-$
4b; X = $N_3^-$
py = 2-pyridyl

## Experimental Section

**Materials and Methods.** Reagents and solvents used were of commercially available reagent quality. Purification of the ligand L'-OH was effected by using flash chromatography[26] with silica gel (60–200 mesh, MCB). Fractions from column chromatography were monitored by using Baker-Flex 1B-F TLC plates with 70% ethanol (190 proof)/30% ethyl acetate. The identity and purity of the ligand L'-OH was judged by TLC, $^1H$ NMR, and mass spectroscopy. All elemental analyses were performed by Galbraith Laboratories, Inc., Knoxville, TN. Infrared and electronic absorption spectra were recorded with PE283 and DMS90 instruments, respectively. $^1H$ NMR spectra were recorded on a Varian EM 360A 360-MHz spectrometer. Chemical shifts are reported as $\tau$ values downfield from an internal standard of $Me_4Si$. Mass spectra were recorded on an AEI MS902 mass spectrometer in the EI mode at 70 eV. Electrical conductivity measurements were carried out in dimethylformamide (DMF) with an Industrial Instruments Inc. conductivity bridge. The cell constant was determined with use of a standard aqueous solution of KCl. Onsager plots[27] were made with use of at least four measurements of the conductance over the concentration range $10^{-3}$–$10^{-5}$ M of copper complex.

The EPR spectra of frozen solutions of several $Cu(L'\text{-}O^-)$ complexes (**3a,b**) and copper bis(2-(2-pyridyl)ethyl)amine complexes (**4a,b**) in $DMF/CHCl_3$ (1:1 ratio) were obtained with a Varian E-4 spectrometer equipped with a liquid-nitrogen Dewar insert. Frozen-solution EPR spectra were obtained at 77 K, and $g$ values were calculated by using a diphenylpicrylhydrazyl (DPPH) calibrant.

**Synthesis of Ligands and Complexes. $[(L\text{-}O^-)Cu_2(Cl)](BPh_4)_2\cdot CH_3C(O)CH_3$ (2a).** Compound **1**[20] (1.0 g, 0.995 mmol) was dissolved in 130 mL of acetone to yield a green solution. 2,2-Dimethoxypropane (2–3 mL) was then added to the solution followed by the dropwise addition of 10.5 mL of a 0.1 M aqueous HCl solution. Addition of the acid resulted in the immediate formation of a dark brown solution, to which an acetone solution of sodium tetraphenylborate (0.95 g, 0.028 mol) was then added. The resulting solution was stirred, and upon layering with dry diethyl ether and standing several days 1.3 g (96% yield) of **2a** was obtained. Anal. Calcd (Found) for $C_{87}H_{85}N_6B_2ClCu_2O$: C, 73.03 (72.88); H, 5.98 (6.15); N, 5.87 (5.82); Cl, 2.48 (2.19). UV/vis ($CH_3CN$; $\lambda_{max}$, nm ($\epsilon$, $M^{-1}$ $cm^{-1}$)): 450 (2140). Molar conductivity: $\Lambda_m$ = 95.0 $\Omega^{-1}$ $cm^2$ $mol^{-1}$.

**$[(L\text{-}O^-)Cu_2(N_3)](PF_6)_2$ (2b).** Compound **1** (1.0 g, 0.995 mmol) was suspended in 175 mL of freshly distilled methanol, to which was added 4–5 mL of 2,2-dimethoxypropane. $Me_3SiN_3$ (0.172 g, 0.149 mmol) in 10 mL of methanol was then added dropwise while the mixture was stirred, and the resulting brown solution was stirred overnight. Dry diethyl ether was layered on the solution, and upon standing 0.39 g (77% yield) of **2b** was obtained. Complex **2b** may also be synthesized by using this same procedure, with either sodium azide or potassium azide as the $N_3^-$ source. Anal. Calcd (Found) for $C_{37}H_{43}N_9Cu_2F_{12}O_2P_2$: C, 41.84 (41.71); H, 4.08 (4.08); N, 11.86 (11.81). IR (Nujol; $cm^{-1}$): $\nu_{N_3}$ 2068. UV/vis ($CH_3CN$; $\lambda_{max}$, nm ($\epsilon$, $M^{-1}$ $cm^{-1}$)): 370 (2600), 460 (3300), 650 (440). Molar conductivity: $\Lambda_m$ = 137 $\Omega^{-1}$ $cm^2$ $mol^{-1}$. Slope from Onsager plot: 260.

**2-(Bromomethyl)phenyl Acetate.** A modification of the published procedure[28] was used. *o*-Cresol (15 g) in acetic anhydride/pyridine (40 mL, 1:1) was allowed to stand for 24 h at room temperature. Removal of solvent followed by distillation afforded the ester (18 g), bp 83 °C (20

(7) Dori, Z.; Ziolo, R. F. *Chem. Rev.* **1973**, *73*, 247.
(8) Agnus, Y.; Louis, R.; Weiss, R. *J. Am. Chem. Soc.* **1979**, *101*, 3381.
(9) Drew, M. G. B.; McCann, M.; Nelson, S. M. *J. Chem. Soc., Chem. Commun.* **1979**, 481.
(10) Comarmond, J.; Plumeré, P.; Lehn, J.-M.; Agnus, Y.; Louis, R.; Weiss, R.; Kahn, O.; Morgenstern-Badarau, I. *J. Am. Chem. Soc.* **1982**, *104*, 6330.
(11) Pickardt, J. *Z. Naturforsch., B: Anorg. Chem., Org. Chem.* **1982**, *37*, 110.
(12) Drew, M. G. B.; Nelson, J.; Esho, F.; McKee, V.; Nelson, S. M. *J. Chem. Soc., Dalton Trans.* **1982**, 1837.
(13) (a) McKee, V.; Dagdigian, J. V.; Bau, R.; Reed, C. A. *J. Am. Chem. Soc.* **1981**, *103*, 7000. (b) McKee, V.; Zvagulis, M.; Dagdigian, J. V.; Patch, M. G.; Reed, C. A. *Ibid.* **1984**, *106*, 4765–4772.
(14) (a) Sorrell, T. N.; O'Connor, C. J.; Anderson, O. P.; Reibenspies, J. H. *J. Am. Chem. Soc.* **1985**, *107*, 4199–4206. (b) Sorrell, T. N. In *Biological & Inorganic Copper Chemistry*; Karlin, K. D., Zubieta, J., Eds.; Adenine: Guilderland, NY, 1986; pp 41–55.
(15) (a) Felthouse, T. R.; Hendrickson, D. N. *Inorg. Chem.* **1978**, *17*, 444. (b) Ziolo, R. F.; Gaugham, Dori, Z.; Pierpont, C. G.; Eisenberg, R. *Ibid.* **1971**, *10*, 1289.
(16) Karlin, K. D.; Hayes, J. C.; Hutchinson, J. P.; Zubieta, J. *J. Chem. Soc., Chem. Commun.* **1983**, 376–378.
(17) Karlin, K. D.; Cohen, B. I. *Inorg. Chim. Acta* **1985**, *107*, L17–L20.
(18) Karlin, K. D.; Farooq, A.; Hayes, J. C.; Cohen, B. I.; Zubieta, J., submitted for publication in *Inorg. Chem.*
(19) Suzuki, M.; Kanatomi, H.; Demura, Y.; Murase, I. *Bull. Chem. Soc. Jpn.* **1984**, *57*, 1003–1007.
(20) Karlin, K. D.; Hayes, J. C.; Gultneh, Y.; Cruse, R. W.; McKown, J. W.; Hutchinson, J. P.; Zubieta, J. *J. Am. Chem. Soc.* **1984**, *106*, 2121–2128.
(21) Karlin, K. D.; Gultneh, Y. *J. Chem. Educ.* **1985**, *62*, 983–990.
(22) Karlin, K. D.; Cruse, R. W.; Gultneh, Y.; Hayes, J. C.; McKown, J. W.; Zubieta, J. In *Biological & Inorganic Copper Chemistry*; Karlin, K. D., Zubieta, J., Eds.; Adenine: Guilderland, NY, 1986; pp 101–114.
(23) Karlin, K. D.; Cruse, R. W.; Gultneh, Y.; Hayes, J. C.; Zubieta, J. *J. Am. Chem. Soc.* **1984**, *106*, 3372.
(24) Karlin, K. D.; Haka, M. S.; Cruse, R. W.; Gultneh, Y. *J. Am. Chem. Soc.* **1985**, *107*, 5828.
(25) Karlin, K. D.; Gultneh, Y. *Prog. Inorg. Chem.*, in press.
(26) Still, W. C.; Kahn, M.; Mitra, A. *J. Org. Chem.* **1978**, *43*, 2923–2925.
(27) (a) Feltham, R. D.; Hayter, R. J. *J. Chem. Soc.* **1964**, 4587–4591. (b) Geary, W. J. *Coord. Chem. Rev.* **1971**, *7*, 81–122.
(28) Range, R. *Tetrahedron* **1971**, *27*, 1499–1502.

mm). $^1$H NMR ($CDCl_3$; $\tau$): 3.0 (m, 4 H), 7.80 (s, 3 H), 7.88 (s, 3 H). IR (neat film; $cm^{-1}$): 1760. Bromination of this ester (10 g) was carried out by refluxing in $CCl_4$ for 1 h with *N*-bromosuccinimide (11.9 g) in the presence of a trace dibenzoyl peroxide. After 1 h, the mixture was cooled and filtered and the solvent removed in vacuo to give an oil, which was distilled to give 2-(bromomethyl)phenyl acetate (5 g), bp 88 °C (0.03 mm). $^1$H NMR ($CDCl_3$; $\tau$): 2.9 (m, 4 H), 5.67 (s, 2 H), 7.78 (s, 3 H).

**L'-OH.** The compound 2-(bromomethyl)phenyl acetate (0.02 mol, 5.12 g), was added to a solution of bis(2-(2-pyridyl)ethyl)amine (py2)[29] (0.022 mol, 5.10 g) and triethylamine (0.05 mol, 5.2 g) in 75 mL of ethyl acetate solution. The mixture was allowed to stir at room temperature for 5 days, whereupon the solution was filtered, and removal of the solvent from the filtrate gave a crude oil, which was found to be a mixture of L'-OAc (80%, $R_f$ 0.65) and L'-OH (20%, $R_f$ 0.46) as determined by $^1$H NMR. This crude mixture was allowed to stir with 100 mL of distilled water, 200 mL of methanol, and 100 mL of a saturated sodium bicarbonate solution at room temperature for 3 h.[30] Addition of an excess of 20% NaOH (aqueous), extraction into dichloromethane, drying over $MgSO_4$ and removal of the solvent gave a crude oil. This was chromatographed on silica gel with 70% EtOH (190 proof)/30% ethyl acetate ($R_f$ = 0.46), and a total of 5.69 g of pure product, L'-OH (**3**), was recovered (76%). $^1$H NMR ($CDCl_3$; $\tau$): 1.9 (m, 2 H), 2.6–3.7 (m, 10 H), 6.4 (s, 2 H), 7.2 (s, 8 H). Mass spectrum (*m/e*): 333 ($M^+$, 8), 241 (33), 226 (29), 135 (100), 121 (16), 107 (50), 93 (21), 79 (13).

**[(L'-O$^-$)Cu(Cl)]·2H$_2$O (3a).** L'-OH (**3**) (1.0 g, 3.0 mmol) and 0.52 g (3.0 mmol) of $CuCl_2 \cdot 2H_2O$ along with 0.12 g (3.0 mmol) of sodium hydroxide were dissolved in a total of 75 mL of methanol and allowed to stir for 30 min. A very dark brown solution developed. An excess of diethyl ether was added to give a crude precipitate, which was recrystallized from MeOH–ether. Filtering and drying the resulting solid in vacuo gave 0.83 g (64%) of brown crystalline material. Anal. Calcd (Found) for $C_{21}H_{26}N_3ClCuO_3$: C, 53.90 (53.46); H, 5.62 (5.73); N, 8.98 (8.86). UV/vis ($CH_3CN$; $\lambda_{max}$, nm ($\epsilon$, $M^{-1}$ $cm^{-1}$)): 260 (11 200), 290 (sh, 5220), 440 (1940), 670 (220) nm. Molar conductivity: $\Lambda_m$ = 38 $\Omega^{-1}$ $cm^2$ $mol^{-1}$. EPR: $g_\parallel$ = 2.25, $g_\perp$ = 2.04, $A_\parallel$ = 147.0 × $10^{-4}$ $cm^{-1}$.

**[(L'-O$^-$)Cu(N$_3$)]·H$_2$O (3b).** A 0.50-g (3.5-mmol) amount of **3a** and 0.023 g (3.5 mmol) of $NaN_3$ was added with 35 mL of MeOH and stirred for 30 min. Precipitation of a dark precipitate was effected by addition of diethyl ether. Recrystallization of this crude material from dichloromethane/ether gave 0.46 g (85%) of black crystalline material. Anal. Calcd (Found) for $C_{21}H_{24}N_6CuO_2$: C, 55.31 (55.76); H, 5.32 (5.00); N, 18.42 (18.10). IR (Nujol; $cm^{-1}$): $\nu_{N_3}$ 2041 $cm^{-1}$. UV/vis ($CH_3CN$; $\lambda_{max}$, nm ($\epsilon$, $M^{-1}$ $cm^{-1}$)): 240 (11 400), 280 (sh, 5280), 405 (2310), 465 (sh, 1380), 650 (260). Molar conductivity: $\Lambda_m$ = 16.0 $\Omega^{-1}$ $cm^2$ $mol^{-1}$. EPR: $g_\parallel$ = 2.23, $g_\perp$ = 2.04, $A_\parallel$ = 156 × $10^{-4}$ $cm^{-1}$.

**(py2)Cu(NO$_3$)$_2$ (4a).** py2 (0.5 g, 2.2 mmol) and 0.53 g (2.2 mmol) of $[Cu^{II}(NO_3)_2] \cdot 3H_2O$ were dissolved in a total of 75 mL of methanol and allowed to stir for 30 min whereupon a dark blue solution developed. An excess of diethyl ether was added to give a crude precipitate, which was recrystallized from MeOH/ether. Filtering and drying the solid in vacuo gave 0.80 g (88%) of blue crystalline material. Anal. Calcd (Found) for $C_{24}H_{17}N_5CuO_6$: C, 40.53 (40.47); H, 4.10 (4.26); N, 16.88 (16.63). UV/vis ($CH_3CN$; $\lambda_{max}$, nm ($\epsilon$, $M^{-1}$ $cm^{-1}$)): 260 (17 100), 290 (sh, 7240), 630 (90). IR (KBr; $cm^{-1}$): $\nu_{NO_3}$ ca. 1380 $cm^{-1}$, $\nu_{NH}$ 3230. Molar conductivity: $\Lambda_m$ = 100 $\Omega^{-1}$ $cm^2$ $mol^{-1}$. EPR: $g_\parallel$ = 2.23, $g_\perp$ = 2.05, $A_\parallel$ = 167 × $10^{-4}$ $cm^{-1}$.

**(py2)Cu(NO$_3$)(N$_3$) (4b).** Complex **4a** (0.2 g (4 mmol), (py2)Cu$(NO_3)_2$) and 0.04 g (4 mmol) of sodium azide were added in a total of 40 mL of $CH_3CN$. Sodium azide was added as a solid, and the solution was allowed to stir for 24 h as a dark green solution developed. An excess of diethyl ether was added to give a crude precipitate, which was recrystallized from $CH_3CN$/ether. Filtering and drying the solid in vacuo gave 0.14 g (79%) of dark black crystalline material. Anal. Calcd (Found) for $C_{14}H_{17}N_7CuO_3$: C, 42.56 (42.47); H, 4.35 (4.31); N, 24.84 (24.41). UV/vis ($CH_3CN$; $\lambda_{max}$, nm ($\epsilon$, $M^{-1}$ $cm^{-1}$)): 260 (12 470), 285 (sh, 3460), 400 (2340), 640 (330). IR (KBr; $cm^{-1}$): $\nu_{NO_3}$ ca. 1380, $\nu_{N_3}$ 2043, $\nu_{NH}$ 3230. Molar conductivity: $\Lambda_M$ = 76.0 $\Omega^{-1}$ $cm^2$ $mol^{-1}$. EPR: $g_\parallel$ = 2.20, $g_\perp$ = 2.04, $A_\parallel$ = 175 × $10^{-4}$ $cm^{-1}$.

**X-ray Crystallography. Crystallization, Collection, and Reduction of X-ray Diffraction Data.** A dichloromethane/diethyl ether solution of compound **2b** standing at 0 °C yielded needle-shaped green crystals that were suitable for X-ray crystallographic analysis. Brown X-ray-quality (needle-shaped) crystals of the compound **3b** were obtained from methanol/diethyl ether at 0 °C. Epoxy-covered crystals (of both **2b** and **3b**) were mounted on a Nicolet R3m four-circle automated diffractometer with a Mo X-ray source equipped with a highly ordered graphite monochromator (λ(Mo Kα) = 0.710 73 Å). Automatic centering and least-squares routines were carried out on 25 reflections for compound **2b** and 15 reflections for compound **3b** to obtain the cell dimensions that are given in Table I. A coupled θ(crystal)–2θ(counter) scan mode was employed. The scan length was $(2\theta(K\alpha_1 - 1.0))-(2\theta(K\alpha_2 + 1.0))°$. Three check reflections were measured every 197 reflections; these exhibited no significant decay during data collection. The program XTAPE of the SHELXTL package[31] was used to process the data in both complexes. A summary of cell parameters, data collection parameters, and refinement results for complexes **2b** and **3b** is found in Table I. In spite of repeated attempts to grow larger crystals of **3b**, only small fine crystals could be obtained; collection of data and structure solution were undertaken with the best crystal available.

**Table I.** Crystallographic Data for Complexes **2b** and **3b**

| | **2b** | **3b** |
|---|---|---|
| **Crystallographic Data** | | |
| temp, K | 294 | 294 |
| *a*, Å | 9.583 (1) | 9.529 (7) |
| *b*, Å | 10.123 (2) | 18.950 (21) |
| *c*, Å | 23.758 (4) | 13.829 (5) |
| α, deg | 87.19 | 90.00 |
| β, deg | 88.83 (1) | 109.38 (5) |
| γ, deg | 84.85 (1) | 90.00 |
| *V*, Å$^3$ | 2292.5 | 2355.7 |
| *F*(000) | 1128 | 1004 |
| *Z* | 2 | 4 |
| $D_{calcd}$, g/cm$^3$ | 1.62 | 1.36 |
| space group | $P\bar{1}$ | $P2_1/c$ |
| cryst dimens, mm | 0.16 × 0.20 × 0.16 | 0.11 × 0.20 × 0.14 |
| scan rate, deg/min | 7.0–30.0 | 7.0–30.0 |
| scan range, deg | 2.0–45.0 | 2.0–35.0 |
| bkgd measmt | stationary cryst, stationary counter, at the beginning and end of each 2θ scan, each for the time taken for the scan | |
| reflecns measd | $+h,\pm k,\pm l$ | $+h,+k,\pm l$ |
| reflecns collected | 6575 | 1762 |
| indep reflecns | 3077 ($\geq 4\sigma\|F_o\|$) | 782 ($\geq 6\sigma\|F_o\|$) |
| abs coeff, cm$^{-1}$ | 12.50 | 9.67 |
| **Reduction of Intensity Data and Summary of Structure Solution and Refinement**[a] | | |
| agreement between equiv reflecns | 0.021 | 0.024 |
| abs cor | not applied | not applied |
| $T_{max}/T_{min}$ | 1.07 | 1.08 |
| atom scattering factors[b] | neutral atomic scattering factors used throughout anal. | |
| anomalous dispersion[c] | applied to all non-H atoms | |
| $R$[d] | 0.0750 | 0.0801 |
| $R_w$[d] | 0.0734 | 0.0814 |
| goodness of fit[e] | 1.709 | 2.226 |

[a] Data were corrected for background, attenuators, and Lorentz and polarization effects in the usual fashion. Hyde, J.; Venkatasubramanian, K.; Zubieta, J. *Inorg. Chem.* **1978**, *17*, 414. [b] Cromer, D. T.; Mann, J. B. *Acta Crystallogr., Sect. A: Cryst. Phys., Diffr., Theor. Gen. Crystallogr.* **1968**, *A24*, 321. [c] *International Tables for X-ray Crystallography*; Kynoch: Birmingham, England, 1962; Vol, III. [d] $R = \sum[|F_o| - |F_c|]/\sum|F_o|$; $R_w = [\sum w(|F_o| - |F_c|)^2/\sum w|F_o|^2]^{1/2}$; $w = 1/\delta^2(F_o) + g(F_o)^2$; $g$ = 0.001. [e] GOF = $[\sum w(|F_o| - |F_c|)^2/(NO - NV)]^{1/2}$, where NO is the number of observations and NV is the number of variables.

**Structure Solution and Refinement of 2b.** The positional parameters of the copper atoms were determined by the Patterson method. A series of difference Fourier maps revealed the positions of the remaining non-hydrogen atoms. All non-hydrogen atoms were refined anisotropically. The hydrogen atoms were included in the final stages of refinement. Their isotropic thermal parameters were 1.2 times those of the carbons to which they were bonded. Carbon–hydrogen bond distances were fixed at 0.96 Å. The two hexafluorophosphate anions were observed to be

(29) (a) Romary, J. K.; Zachariasen, R. D.; Garger, J. D.; Schiesser, H. *J. Chem. Soc. C* **1968**, 2884–2887. (b) Nelson, S. M.; Rodgers, J. *Inorg. Chem.* **1967**, *6*, 1390–1395.

(30) Bache, G.; Wienrab, S. M. *J. Am. Chem. Soc.* **1971**, *93*, 746–752.

(31) All calculations were performed on a Data General Nova 3 computer with 32K of 16-bit words using local versions of the Nicolet SHELXTL interactive crystallographic software package, as described in: Sheldrick, G. M. *Nicolet SHELXTL Operations Manual*; Nicolet XRD Corp.: Cupertino, CA, 1979.

**Table II.** Selected Bond Distances and Angles for **2b** and **3b**

| 2b | | 3b | |
|---|---|---|---|
| | Interatomic Distances (Å) | | |
| Cu1–O1 | 1.963 (8) | Cu1–O1 | 1.928 (14) |
| Cu1–N2 | 1.985 (10) | Cu1–N1 | 2.127 (23) |
| Cu1–N7 | 2.024 (12) | Cu1–N2 | 2.027 (16) |
| Cu2–N4 | 2.048 (9) | Cu1–N3 | 2.162 (24) |
| Cu2–N6 | 2.141 (10) | Cu1–N4 | 2.004 (26) |
| N7–N8 | 1.117 (21) | N4–N5 | 1.219 (34) |
| Cu1–N1 | 2.057 (10) | N5–N6 | 1.231 (41) |
| Cu1–N3 | 2.204 (10) | | |
| Cu2–O1 | 1.976 (8) | | |
| Cu2–N5 | 2.001 (10) | | |
| Cu2–N7 | 2.028 (12) | | |
| N8–N9 | 1.150 (28) | | |
| Cu1–Cu2 | 3.185 (3) | | |
| | Interatomic Angles (deg) | | |
| O1–Cu1–N1 | 94.1 (3) | O1–Cu1–N1 | 95.2 (8) |
| O1–Cu1–N3 | 96.0 (3) | O1–Cu1–N2 | 165.8 (9) |
| N1–Cu1–N2 | 94.9 (4) | O1–Cu1–N3 | 98.1 (7) |
| N1–Cu1–N7 | 155.6 (5) | O1–Cu1–N4 | 79.2 (9) |
| N2–Cu1–N7 | 89.9 (4) | N1–Cu1–N2 | 89.0 (8) |
| O1–Cu2–N4 | 94.2 (3) | N1–Cu1–N3 | 90.6 (9) |
| O1–Cu2–N6 | 94.6 (3) | N1–Cu1–N4 | 165.8 (11) |
| N4–Cu2–N5 | 95.1 (4) | N2–Cu1–N3 | 95.5 (8) |
| N4–Cu2–N7 | 155.5 (5) | N2–Cu1–N4 | 93.7 (9) |
| N5–Cu2–N7 | 91.3 (4) | N3–Cu1–N4 | 103.0 (11) |
| Cu1–O1–Cu2 | 107.9 (3) | N4–N5–N6 | 174.3 (32) |
| Cu2–O1–C7 | 126.4 (7) | Cu1–O1–C1 | 121.1 (17) |
| Cu1–N7–N8 | 130.5 (12) | | |
| N7–N8–N9 | 173.5 (20) | | |
| O1–Cu1–N2 | 158.9 (4) | | |
| O1–Cu1–N7 | 74.4 (4) | | |
| N1–Cu1–N3 | 97.5 (4) | | |
| N2–Cu1–N3 | 101.7 (4) | | |
| N3–Cu1–N7 | 104.9 (4) | | |
| O1–Cu2–N5 | 161.7 (4) | | |
| O1–Cu2–N7 | 74.0 (4) | | |
| N4–Cu2–N6 | 96.9 (4) | | |
| N5–Cu2–N6 | 99.9 (4) | | |
| N6–Cu2–N7 | 105.3 (4) | | |
| Cu1–O1–C7 | 125.7 (7) | | |
| Cu1–N7–Cu2 | 103.6 (5) | | |
| Cu2–N7–N8 | 125.1 (11) | | |

unexceptional, and they possessed the expected bond distances and angles. A solvent of crystallization was located and identified as dichloromethane. A peak of electron density equal to about 1.8 e/Å$^3$ showed up in a nonpopulated region of the final difference Fourier map. Attempts to identify this peak were unsuccessful. Since a reasonable analysis was obtained for this compound, this peak was ignored. The final *R* factors and refinement data appear in Table I. Selected bond distances and angles are presented in Table II. Final positional parameters are given in Table III.

**Structure Solution and Refinement of 3b.** A sharpened Patterson map revealed the position of the copper atom. A series of difference Fourier maps revealed the locations of the remaining non-hydrogen atoms. All of the atoms in the coordinated azide and the atoms in the coordination sphere, with the exception of N2, were refined anisotropically. The hydrogen atoms were included in the final stages of refinement. The carbon–hydrogen bond lengths were set at 0.96 Å, and isotropic thermal parameters were 1.2 times those of the bonded carbons. A methanol of crystallization with an occupancy factor of 0.5 was found to be present, as were three water molecules with the occupancy factors 0.25, 0.50, and 0.75 in the final stages of refinement. Refinement data and final *R* factors are presented in Table I. Selected bond angles and distances are found in Table II. Final positional parameters are given in Table IV.

Structure factors, bond lengths, bond angles, anisotropic temperature factors, and hydrogen coordinates and temperature factors are available in the supplementary material for compounds **2b** (Tables VI–X) and **3b** (Tables XI–XV).

## Discussion

**Description of Structures. $[(L\text{-}O^-)Cu_2(N_3)](PF_6)_2$ (2b).** The two cupric atoms are bridged by an endogenous phenoxo oxygen atom and an exogenous azide ligand, which is coordinated in a $\mu$-1,1 bridging fashion. Each cupric atom is pentacoordinate with ligation to the tridentate py2 unit, the phenoxo oxygen atom, and the azide ligand. The copper atoms are crystallographically independent with a pseudotwofold axis passing through the C4, C7, O1, N7, N8, and N9 atoms (Figure 1).

The coordination geometries of the pentacoordinate cupric compounds **2b** and **3b** can be analyzed and described by using an approach developed by Muetterties and Guggenberger.[32] In

**Table III.** Atom Coordinates (×10$^4$) and Temperature Factors (Å$^2$ × 10$^3$) for Compound **2b**

| atom | *x* | *y* | *z* | $U_{equiv/iso}$[a] |
|---|---|---|---|---|
| Cu1 | 411 (2) | 2761 (2) | 1843 (1) | 43 (1)* |
| Cu2 | 1731 (2) | 3276 (2) | 3023 (1) | 41 (1)* |
| O1 | 2117 (8) | 2458 (7) | 2292 (3) | 39 (3)* |
| N1 | 1466 (10) | 2579 (9) | 1084 (4) | 45 (4)* |
| N2 | −1306 (11) | 3709 (9) | 1514 (4) | 49 (4)* |
| N3 | −185 (10) | 709 (10) | 1942 (4) | 52 (4)* |
| N4 | 3351 (10) | 2175 (9) | 3422 (4) | 41 (4)* |
| N5 | 757 (10) | 3863 (8) | 3733 (4) | 40 (4)* |
| N6 | 2831 (11) | 4984 (9) | 2808 (4) | 52 (4)* |
| N7 | −84 (12) | 3565 (12) | 2592 (5) | 57 (5)* |
| N8 | −1123 (19) | 3932 (14) | 2775 (6) | 93 (7)* |
| N9 | −2198 (22) | 4400 (32) | 2921 (9) | 253 (17)* |
| C1 | 2942 (12) | 2844 (13) | 1165 (5) | 51 (5)* |
| C2 | 3749 (12) | 1932 (13) | 1567 (6) | 48 (5)* |
| C3 | 4996 (14) | 1197 (14) | 1412 (5) | 62 (6)* |
| C4 | 5796 (13) | 443 (15) | 1798 (6) | 70 (6)* |
| C5 | 5378 (14) | 391 (13) | 2347 (5) | 53 (5)* |
| C6 | 4159 (13) | 1019 (11) | 2523 (5) | 40 (5)* |
| C7 | 3332 (12) | 1831 (13) | 2124 (6) | 47 (5)* |
| C8 | 3665 (13) | 893 (11) | 3124 (5) | 45 (5)* |
| C21 | −2585 (14) | 3496 (14) | 1723 (6) | 61 (6)* |
| C22 | −3768 (15) | 4409 (21) | 1583 (7) | 85 (8)* |
| C23 | −3577 (18) | 5410 (14) | 1238 (7) | 86 (8)* |
| C24 | −2303 (16) | 5633 (14) | 1011 (6) | 72 (7)* |
| C25 | −1199 (15) | 4775 (15) | 1148 (5) | 60 (6)* |
| C26 | 227 (15) | 4816 (15) | 895 (5) | 67 (6)* |
| C27 | 812 (15) | 3669 (14) | 641 (5) | 63 (6)* |
| C31 | −440 (14) | 132 (14) | 2447 (5) | 53 (5)* |
| C32 | −744 (15) | −1151 (17) | 2517 (7) | 75 (7)* |
| C33 | −796 (16) | −1906 (14) | 2051 (9) | 79 (8)* |
| C34 | −536 (15) | −1328 (16) | 1534 (7) | 70 (7)* |
| C35 | −243 (12) | −31 (12) | 1481 (5) | 42 (5)* |
| C36 | 18 (15) | 638 (15) | 922 (6) | 68 (6)* |
| C37 | 1449 (15) | 1240 (14) | 863 (5) | 63 (6)* |
| C51 | 82 (15) | 5076 (13) | 3769 (6) | 59 (6)* |
| C52 | −868 (17) | 5368 (19) | 4194 (8) | 82 (8)* |
| C53 | −1123 (18) | 4356 (22) | 4596 (8) | 85 (8)* |
| C54 | −452 (17) | 3206 (17) | 4543 (7) | 70 (7)* |
| C55 | 505 (14) | 2914 (14) | 4128 (6) | 53 (6)* |
| C56 | 1328 (15) | 1633 (13) | 4096 (5) | 57 (6)* |
| C57 | 2928 (13) | 1812 (14) | 4015 (5) | 56 (5)* |
| C61 | 2407 (17) | 5855 (15) | 2386 (6) | 80 (7)* |
| C62 | 3148 (21) | 6832 (14) | 2176 (7) | 83 (8)* |
| C63 | 4328 (25) | 7085 (16) | 2455 (10) | 103 (10)* |
| C64 | 4737 (18) | 6341 (16) | 2898 (8) | 85 (8)* |
| C65 | 3998 (14) | 5204 (12) | 3084 (6) | 51 (5)* |
| C66 | 4396 (15) | 4387 (12) | 3574 (6) | 58 (6)* |
| C67 | 4653 (13) | 2884 (11) | 3432 (5) | 48 (5)* |
| P1 | 7681 (4) | 9512 (4) | 4124 (2) | 67 (2)* |
| P2 | 3073 (4) | −2552 (4) | 279 (2) | 68 (2)* |
| F11 | 9121 (9) | 8788 (11) | 3932 (4) | 120 (5)* |
| F12 | 6224 (10) | 10238 (11) | 4297 (4) | 117 (5)* |
| F13 | 7437 (10) | 8344 (9) | 4572 (4) | 96 (4)* |
| F14 | 8424 (11) | 10242 (11) | 4588 (4) | 123 (5)* |
| F15 | 7924 (12) | 10657 (11) | 3677 (4) | 128 (5)* |
| F16 | 6934 (10) | 8749 (11) | 3678 (4) | 115 (5)* |
| F21 | 1485 (11) | −2177 (11) | 421 (6) | 150 (6)* |
| F22 | 3011 (13) | −1248 (12) | −49 (6) | 171 (7)* |
| F23 | 3518 (18) | −1768 (15) | 770 (5) | 198 (9)* |
| F24 | 3151 (12) | −3775 (13) | 662 (6) | 172 (7)* |
| F25 | 2619 (17) | −3269 (17) | −198 (7) | 237 (10)* |
| F26 | 4638 (11) | −2883 (12) | 111 (5) | 145 (6)* |
| Cl1 | 2528 (5) | 7846 (5) | 4105 (2) | 113 (2)* |
| Cl2 | 4591 (6) | 6562 (5) | 4848 (3) | 124 (3)* |
| C | 3960 (18) | 8027 (19) | 4517 (8) | 113 (10)* |

[a] Values marked with asterisks are equivalent isotropic *U* values defined as one-third of the trace of the orthogonalized $U_{ij}$ tensor.

**Table IV.** Atom Coordinates ($\times 10^4$) and Temperature Factors (Å$^2$ $\times 10^3$) for Compound **3b**

| atom | x | y | z | $U_{equiv/iso}$[a] |
|---|---|---|---|---|
| Cu | 2536 (4) | 1133 (2) | 3344 (3) | 38 (1)* |
| O1 | 4344 (18) | 1093 (11) | 4505 (12) | 53 (8)* |
| N1 | 2862 (23) | 2187 (12) | 2935 (15) | 46 (11)* |
| N2 | 921 (20) | 1019 (11) | 1964 (14) | 38 (6) |
| N3 | 1065 (23) | 1500 (11) | 4138 (14) | 50 (10)* |
| N4 | 2678 (31) | 95 (14) | 3635 (19) | 76 (15)* |
| N5 | 1934 (28) | -326 (14) | 3005 (19) | 59 (14)* |
| N6 | 1207 (37) | -793 (19) | 2439 (25) | 99 (19)* |
| C1 | 4924 (31) | 1649 (16) | 5029 (22) | 47 (8) |
| C2 | 5544 (29) | 1615 (18) | 6096 (22) | 65 (10) |
| C3 | 6327 (30) | 2186 (14) | 6682 (21) | 52 (9) |
| C4 | 6474 (33) | 2827 (16) | 6231 (23) | 78 (10) |
| C5 | 5847 (33) | 2927 (19) | 5137 (23) | 93 (12) |
| C6 | 5064 (27) | 2310 (15) | 4532 (18) | 36 (8) |
| C7 | 4428 (27) | 2365 (14) | 3379 (17) | 39 (8) |
| C21 | -322 (27) | 690 (13) | 1880 (19) | 39 (8) |
| C22 | -1384 (28) | 540 (14) | 936 (18) | 48 (9) |
| C23 | -1031 (27) | 714 (14) | 99 (20) | 44 (8) |
| C24 | 193 (27) | 1021 (13) | 132 (19) | 53 (8) |
| C25 | 1254 (26) | 1155 (15) | 1097 (18) | 45 (8) |
| C26 | 2613 (27) | 1556 (14) | 1287 (19) | 48 (9) |
| C27 | 2543 (32) | 2247 (14) | 1808 (21) | 55 (9) |
| C31 | 893 (26) | 1053 (15) | 4875 (18) | 53 (8) |
| C32 | -114 (29) | 1183 (17) | 5406 (20) | 69 (9) |
| C33 | -979 (30) | 1759 (14) | 5129 (21) | 58 (10) |
| C34 | -851 (29) | 2195 (15) | 4357 (19) | 50 (9) |
| C35 | 136 (30) | 2067 (14) | 3871 (20) | 48 (8) |
| C36 | 373 (28) | 2518 (14) | 3062 (19) | 44 (9) |
| C37 | 1929 (27) | 2699 (14) | 3276 (20) | 47 (9) |
| O2 | 5000 | 5000 | 0 | 88 (7) |
| O4 | 5129 (50) | 9528 (27) | 1294 (35) | 116 (17) |
| C(sol) | 3308 (63) | 5459 (33) | 1835 (43) | 70 (20) |
| O5 | 3843 (42) | 4964 (23) | 1567 (30) | 92 (14) |
| O3 | 5000 | 0 | 0 | 125 (26) |

[a] Values marked with asterisks are equivalent isotropic $U$ values defined as one-third of the trace of the orthogonalized $U_{ij}$ tensor.

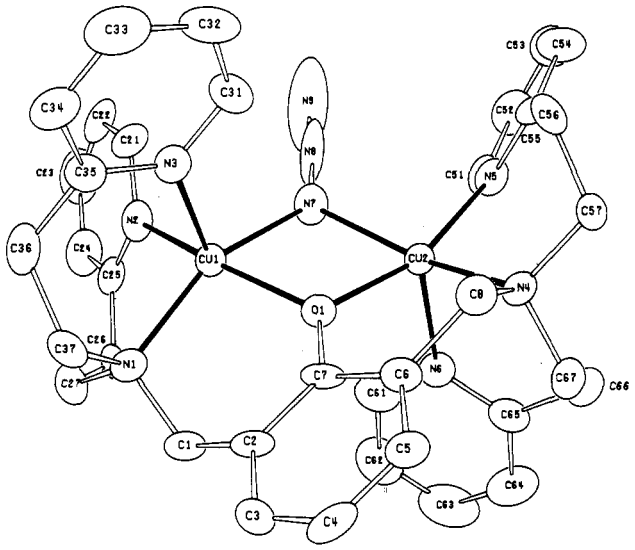


**Figure 1.** ORTEP diagram for the $\mu$-1,1-azido-bridged dicopper(II) complex **2b** showing the atom-labeling scheme.

this method, the important dihedral angles (known as the shape-determining angles, $e_1$, $e_2$, and $e_3$) can be calculated in order to describe a complex geometry. The two possible limiting geometries for a five-coordinate metal center are square-base pyramidal (SP) and trigonal bipyramidal (TBP). The key shape-determining angle is $e_3$, which is 0.0° for SP complexes and 53.0° for TBP complexes. As applied to compound **2b**, the Muetterties and Guggenberger analysis yields the shape-determining angles 6.8° for Cu1 and 9.8° for Cu2. Thus, the coordination geometry around each copper ion can best be described as slightly distorted SP. The basal ligand atoms around Cu1 are N1, N2, O1, and N7, while those for Cu2 are N4, N5, O1, and N7. Atoms N3 and N6 are found to occupy the axial positions for Cu1 and Cu2, respectively. Atoms Cu1 and Cu2 are displaced 0.31 and 0.32 Å, respectively, out of their corresponding basal planes in a direction toward the axial pyridyl groups. The $Cu_2(O1(N7)$ units is nearly planar with the maximum deviation of any of the four atoms from the best least-squares plane being 0.016 Å.

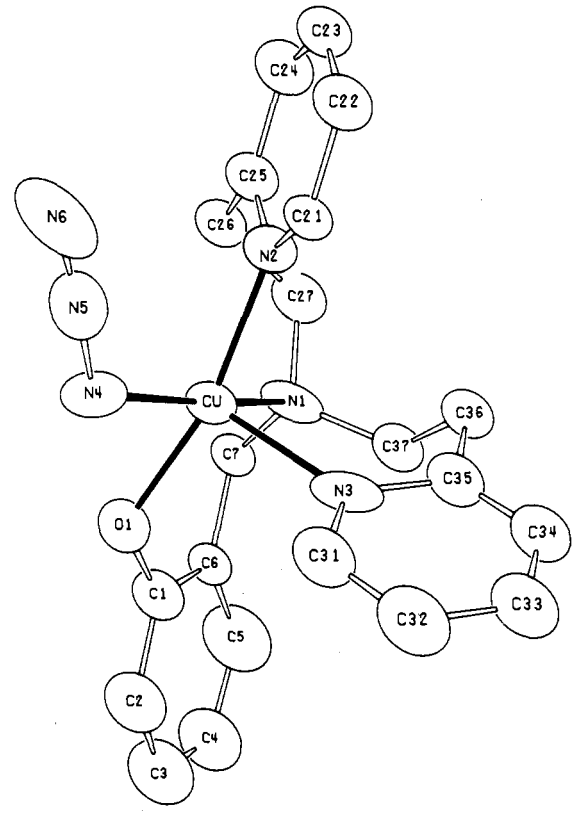


**Figure 2.** ORTEP diagram for the azido-coordinated monomeric copper(II) complex **3b** showing the atom-labeling scheme.

The copper–ligand bond lengths for **2b** are in the range seen for other related pentacoordinate cupric compounds with similar ligands. Equatorial Cu–$N_{py}$ distances are Cu1–N2 = 1.985 (10) Å and Cu2–N5 = 2.001 (10) Å. Cu–$N_{amine}$ distances are Cu1–N1 = 2.057 (10) Å and Cu2–N4 = 2.048 (9) Å while the remaining equatorial bond lengths are Cu1–O1 = 1.963 (8) Å, Cu1–N7 = 2.024 (12) Å, Cu2–O1 = 1.976 (8) Å, and Cu2–N7 = 2.028 (12) Å. As expected and as seen previously,[20] the axial Cu–$N_{py}$ bond distances are elongated, Cu1–N3 = 2.204 (10) Å and Cu2–N6 = 2.141 (10) Å. The Cu···Cu separation of 3.185 (3) Å is greater than that observed for the analogous hydroxo-bridged precursor complex, **1** (Cu···Cu = 3.08 Å) and is accompanied by a corresponding increase in the Cu–O1–Cu angle from 104.4 (5)° in **1** to 107.9 (3)° in **2b**. The dihedral angle between the planes defined by O1/Cu1/N7 and O1/Cu/N7 is 2.3°. The angle between the planes defined by N2/N1/N7/O1 and N7/O1/N4/N5 is 8.1° with Cu1 0.3187 Å above this basal plane and Cu2 0.3478 Å below its basal plane (Figure 1).

**$[(L'\text{-}O^-)Cu(N_3)]\cdot H_2O$ (3b).** This complex is a neutral species that is a mononuclear analogue to **2b**. The cupric atom is coordinated to two pyridyl nitrogen atoms, an amine nitrogen atom, and a phenoxo oxygen atom from the tetradentate ligand. Pentacoordination is achieved through ligation to the terminal azide ligand. The copper(II) coordination geometry is almost an ideal square-based pyramid (SP); a shape-determining angle $e_3$ = 0.9° is found. Atoms N1, N2, O1, and N4 (Figure 2) make up the basal plane and the pyridyl nitrogen, N3, occupies the axial position in the coordination sphere. The cupric ion lies 0.23 Å

(32) Muetterties, E. L.; Guggenberger, L. J. *J. Am. Chem. Soc.* **1974**, *96*, 1748–1756.

**Table V.** Charge-Transfer Spectra for Compounds **2–4**

| compd | λ, nm | ε, $M^{-1}$ $cm^{-1}$ | assignt |
|---|---|---|---|
| $[(L\text{-}O^-)Cu_2(Cl)]\cdot CH_3C(O)CH_3$ (**2a**) | 450 | 2140 | $PhO^- \rightarrow Cu(II)$ |
| $[(L\text{-}O^-)Cu_2(N_3)]$ (**2b**) | 460 | 3300 | $PhO^- \rightarrow Cu(II)$ |
| | 370 | 2600 | $N_3^- \rightarrow Cu(II)$ |
| $[(L'\text{-}O^-)Cu(Cl)]\cdot 2H_2O$ (**3a**) | 440 | 1940 | $PhO^- \rightarrow Cu(II)$ |
| $[(L'\text{-}O^-)Cu(N_3)]\cdot H_2O$ (**3b**) | 465 sh | 1380 | $PhO^- \rightarrow Cu(II)$ |
| | 405 | 2310 | $N_3^- \rightarrow Cu(II)$ |
| $[(py2)Cu(NO_3)_2]$ (**4a**) | ... | ... | ... |
| $[(py2)Cu(NO_3)(N_3)]$ (**4b**) | 400 | 2340 | $N_3^- \rightarrow Cu(II)$ |

above this basal plane in the direction of N3. In the basal plane, N1 is trans to N4 (N1–Cu–N4 = 165.8 (11)°) and O1 is trans to N2 (O1–Cu–N2) = 165.8 (9)°). Equatorial copper–ligand bond lengths are Cu–N1 = 2.127 (23) Å, Cu–N2 = 2.027 (16) Å, Cu–O1 = 1.928 (14) Å, and Cu–N4 = 2.004 (26) Å while the axial bond length is Cu–N3 = 2.162 (24) Å.

Comparison of the structural parameters for **2b** and **3b** reveals that, except for minor differences, the two compounds are essentially structurally identical with respect to the coordination geometry about Cu(II) (Table II). For **3b**, Cu–O1–C1 = 122.1 (17)° and Cu–N4–N5 = 120.9 (19)° as compared to Cu1–O1–C7 = 125.7 (7)°, Cu1–N7–N8 = 130.5 (12)°, Cu2–O1–C7 = 126.4 (7)°, and Cu2–N7–N8 = 125.1 (11)° for **2b**. The azido ligands in both **2b** and **3b** are nearly linear with N7–N8–N9 = 173.5 (20)° and N4–N5–N6 = 174.3 (32)°, respectively.

**Electronic Spectral Assignments.** Comparison of the electronic spectral features in complexes **2–4** allows us to assign with some confidence those ligand-to-metal charge-transfer (LMCT) transitions in the visible region due to the coordinated phenoxo and/or azide ligands in **2** and **3** (Table V). Derivatives **4**, containing the tridentate py2 ligand, were synthesized in order to check the effect of this amine–pyridine-containing donor group in the absence of both phenoxo and azide ligands (**4a**) or in the presence of only a single $N_3^-$ ligand (**4b**). It should be noted that Cu(II) is found to be in a tetragonal environment in all of these complexes, as judged by the solid-state structures determined for **2a**, **2b**, and **3b** (SP coordination geometry) and the axial solution EPR spectra observed for compounds **3b**, **4a**, and **4b** (see Experimental Section).

The assignments are based on the following observations. (a) The synthesis of chloride analogues **2a** and **3a** and the observation of their electronic spectral properties allow us to assign the phenoxo-to-Cu(II) LMCT band since we have found that coordinated $Cl^-$ gives rise to only very weak or nonobservable absorptions in the region of interest for these systems.[17,33] (b) $Cu(py2)(NO_3)_2$ (**4a**) shows no visible bands in the 300–600-nm region; thus, any absorptions in other complexes containing $Cl^-$, $N_3^-$, or $PhO^-$ can be monitored easily. The nitrate ligand bound to Cu(II) also contributes no absorption in the 300–600-nm region. (c) With azide and py2 coordinated to Cu(II) (complex **4b**), a band at 400 nm ($\epsilon$ = 2340 $M^{-1}$ $cm^{-1}$) appears, providing a "baseline" marker for a $N_3^- \rightarrow$ Cu(II) LMCT transition. (d) Thus, the electronic spectra observed for complexes **3a** (X = $Cl^-$) and **3b** (X = $N_3^-$) suggest that $PhO^- \rightarrow$ Cu(II) transitions occur close to 450 nm while that for $N_3^- \rightarrow$ Cu(II) is found nearer 400 nm (Table V). (e) Similarly, only one band is seen in the chloride- and phenoxo-bridged dicopper(II) species **2a**, while two absorptions are observed in **2b**, which possesses both phenoxo and azide ligands bridged to Cu(II). The lower energy absorption can again be assigned to the phenoxo-to-Cu(II) LMCT transition by analogy to the monomeric complexes.

Thus, we can summarize our spectral assignments on the basis of the arguments described above (Table V). For complexes **2a** and **3a**, a single absorption in the CT region is observed at 450 ($\epsilon$ = 2140 $M^{-1}$ $cm^{-1}$) and 440 nm ($\epsilon$ = 1940 $M^{-1}$ $cm^{-1}$), respectively. Thus, these bands are assigned to $PhO^- \rightarrow$ Cu(II) transitions. The dinuclear azide complex **2b** exhibits LMCT bands at 370 nm ($\epsilon$ = 2600 $M^{-1}$ $cm^{-1}$) and 460 nm ($\epsilon$ = 3300 $M^{-1}$ $cm^{-1}$) and a d–d envelope at 655 nm. We assign the lower energy band at 460 nm to the $PhO^- \rightarrow$ Cu(II) LMCT transition and the 370-nm band to the $N_3^- \rightarrow$ Cu(II) LMCT transition. The lower energy (465 (sh) nm, ($\epsilon$ = 1380 $M^{-1}$ $cm^{-1}$)) and higher energy (405 nm ($\epsilon$ = 2310 $M^{-1}$ $cm^{-1}$)) bands are given similar assignments for the monomeric analogue **3b**.

## Conclusions

Complexes **3** and others containing L'-OH[17] were synthesized and studied in order to establish the structural and spectral characteristics expected for the simpler mononuclear system and thus enable us to better understand the properties of the dinuclear compounds with L-OH. It is clear that our approach has been successful; the solid-state structure of the mononuclear compound **3b** shows that the Cu(II) coordination environment is very similar to that observed in the dinuclear complexes **2**. It is evident from the spectral assignments that are made in this study that our prior assignment[16] of the azido-to-Cu(II) and phenoxo-to-Cu(II) LMCT bands in **2b** was incorrect and should be reversed. The present study firmly establishes the $PhO^- \rightarrow$ Cu(II) transition to be in the 450–460-nm range for complexes **2** and **3**, and a band is also observed in this region for a number of other X-bridged (X = Br, acetate, benzoate) complexes of the type **2**.[18] The hydroxo-bridged complex **1** seems to be an exception in this regard, since it possesses an absorption maximum at 380 nm, although the absorption envelope does tail considerably to lower energy.[34]

It is interesting to compare the $N_3^- \rightarrow$ Cu(II) LMCT band positions of complexes **2b** and **3b** with those of related complexes and with those of the protein derivatives containing azide. Using a dinucleating ligand analogous to L-OH, but possessing pyrazolyl donor groups instead of pyridine, Sorrell and co-workers[14] have characterized both $\mu$-1,1- and $\mu$-1,3-azido dicopper(II) complexes that are also phenoxo bridged. In the $\mu$-1,1 bridged compound, bands at 462 and 364 nm are assigned to $N_3^- \rightarrow$ Cu(II) and $PhO^- \rightarrow$ Cu(II), respectively, which is inconsistent with our current findings. A survey of a variety of other azide–Cu(II) complexes, some bridged dicopper(II) (both $\mu$-1,1 and $\mu$-1,3 bridging) species and some with terminal coordination, indicates that the azide-to-Cu(II) LMCT transition occurs in the range 360–405 nm.[13,19,35] However, data on azido copper protein derivatives[6,36] indicate that absorptions over a wide range (300–550 nm) can occur, even in cases with apparently similar $\mu$-1,3-$N_3^-$ coordination (*Buscyon* azido–methemocyanin, λ = 380 nm ($\epsilon$ = 1500 $M^{-1}$ $cm^{-1}$), $\nu_{N_3^-}$ = 2042 $cm^{-1}$,[6] Cu···Cu = 3.66 Å;[37] *Limulus* azido–methemocyanin, λ = 500 nm ($\epsilon$ = 500 $M^{-1}$ $cm^{-1}$) and <375 nm (stronger),[6] Cu···Cu = 3.66 Å[37]). Clearly, there are differences in the donor ligands and in the subtleties of the coordination environment of the $N_3^-$ ligand in the complexes and protein derivatives that contribute to the differences in absorption spectra observed. In addition, since multiple LMCT transitions are often observed and expected for bridging ligands such as $N_3^-$,[1,6,36] the spectral analyses and/or assignments made in these systems are undoubtedly too simplified; further in-depth studies and comparisons of spectral features as a function of coordination mode are required. We note in passing that the strong asymmetric IR band observed for copper-coordinated $N_3^-$ occurs in the range 2020–2042 $cm^{-1}$ for terminal or $\mu$-1,3 bridging situations but occurs at higher energy, 2060–2070 $cm^{-1}$, for $\mu$-1,1 bridged azide.[12-14,16-19]

The synthesis and characterization of the monomeric analogues **3** and **4** has allowed for the assignment of LMCT bands in both the mononuclear (**3**) and dinuclear (**2**) complexes. As described above, the coordination environments and geometries in the complexes **2b** and **3b** are very similar. We should note that another observable difference in physical properties of the complexes is

(33) Karlin, K. D.; McKown, J. W.; Hayes, J. C.; Hutchinson, J. P.; Zubieta, J. *Transition Met. Chem. (Weinheim, Ger.)* **1984**, *9*, 405–406.

(34) Pyrz, J. W.; Karlin, K. D.; Sorrell, T. N.; Vogel, G. C.; Que, L., Jr. *Inorg. Chem.* **1984**, *23*, 4581–4584.

(35) (a) Martin, A. E.; Bulkowski, J. E. *J. Am. Chem. Soc.* **1982**, *104*, 1434–1436. (b) Agnus, Y.; Louis, R.; Grisselbrecht, J. P.; Weiss, R. J. *Ibid.* **1984**, *106*, 93–102.

(36) Allendorf, M. D.; Spira, D. J.; Solomon, E. I. *Proc. Natl. Acad. Sci. U.S.A.* **1985**, *82*, 3063–3067.

(37) Spiro, T. G.; Woolery, G. L.; Brown, J. M.; Powers, L.; Winkler, M. E.; Solomon, E. I. In ref 1b, pp 23–42.

a shift in the position of the stretching vibration observed in the infrared region that occurs at 2041 $cm^{-1}$ for the monomer **3b** and that is found at 2068 $cm^{-1}$ for the dinuclear complex **2b**. Variations in the observed LMCT bands (Table V) that are noteworthy are the "shift" of the position of the $N_3^- \rightarrow Cu(II)$ absorption from 370 nm in the **3b** to 405 nm in **2b** and the intensity increase for the $PhO^- \rightarrow Cu(II)$ band at 460–465 nm on going from the mononuclear azide complex to the dinuclear azide complex. This latter intensity increase is not observed for the corresponding chloride-containing compounds **3a** and **2a**. It also has been recently reported that the C–O(phenoxo) stretching vibrations in the resonance Raman spectra for phenoxo-bridged dinuclear Cu(II) complexes are observed at significantly higher frequencies than those of the corresponding mononuclear analogues.[34] Further studies on this and other systems will be necessary to evaluate the significance, if any, of chemical differences and spectroscopic variations observed that may be due to the dinuclear coordination of small molecules compared to that observed in mononuclear analogues.

**Acknowledgment.** We thank the National Institutes of Health (K.D.K., Grant No. GM 28962 and GM 34909) for support of this research.

**Registry No.** **1**, 86593-51-3; **2a**, 105582-79-4; **2b**, 86597-35-5; **3a**, 93532-00-4; **3b**, 105582-80-7; **4a**, 14870-25-8; **4b**, 105582-81-8; *L'*-OH, 97801-58-6; py2, 15496-36-3; $Me_3SiN_3$, 4648-54-8; 2-(bromomethyl)-phenyl acetate, 704-65-4; *o*-cresol, 95-48-7; *o*-tolyl acetate, 533-18-6.

**Supplementary Material Available:** Listings of bond lengths, bond angles, anisotropic temperature factors, and hydrogen coordinates and temperature factors for compounds **2b** (Tables VII–X) and **3b** (Tables XII–XV) (13 pages); listings of structure factors for **2b** (Table VI) and **3b** (Table XI) (23 pages). Ordering information is given on any current masthead page.

---

Contribution from the Department of Chemistry,
University of Florence, Florence, Italy

# Characterization of the Cobalt(II)-Substituted Superoxide Dismutase–Phosphate Systems

L. Banci, I. Bertini,* C. Luchinat, R. Monnanni, and A. Scozzafava

*Received May 16, 1986*

The systems containing $Co_2Zn_2SOD$ or $Co_2Co_2SOD$ and phosphate have been investigated by means of electronic and $^1H$ NMR spectroscopies. It is suggested that the cobalt ion at the copper site is bound to three histidines and one phosphate ion. Histidine-61, which bridges zinc and cobalt or the two cobalt ions, is detached upon addition of phosphate, which probably binds both Arg-141 and the cobalt ion. The shape of the electronic spectrum of the cobalt ion at the zinc site depends on the terminal or bridging mode of His-61.

## Introduction

It has recently been shown that the demetalized erythrocyte copper–zinc superoxide dismutase (SOD) can bind cobalt(II).[1-3] The latter metal ion easily occupies the zinc site to give $E_2Co_2SOD$, where E stands for the empty copper site.[1] This is quite reasonable on account of the similar chemistry of cobalt(II) and zinc(II) and of the success obtained in substituting zinc(II) with cobalt(II) in zinc enzymes.[4]

The $^1H$ NMR spectra of $E_2Co_2SOD$ indicate that the metal ion is bound to three histidines just as in the native enzyme;[5] this is confirmed by the $^1H$ NMR spectra of $Cu^I_2Co_2SOD$[6] and is consistent with the analysis of the $^1H$ NMR of $Cu_2Co_2SOD$.[5] A second pair of cobalt(II) ions is bound by the dimeric $E_2Co_2SOD$ to form $Co_2Co_2SOD$.[2,3] This reaction is reported to be facilitated by the phosphate ion.[3] The interest in this kind of derivative resides in the characterization of apoSOD as metal chelator and in obtaining derivatives containing spectroscopic probes such as cobalt(II) capable of shedding light on the environment of the metal ion. We have shown that high-spin cobalt(II) is an excellent probe for $^1H$ NMR spectra in that it allows the detection of the proton signals of the metal ligands.[4,7] We have therefore attempted to understand further the nature of the interaction of cobalt(II) and the SOD ligands at the copper site. Furthermore, we have tried to understand the role of phosphate in the cobalt-binding process. Therefore, we have investigated the $^1H$ NMR spectra of $Co_2Co_2SOD$ and $Co_2Zn_2SOD$ in the presence of increasing amounts of phosphate at pH 7.4, and we have remeasured the electronic spectra of the two systems as well as $^{31}P$ NMR parameters.

**Chart I**

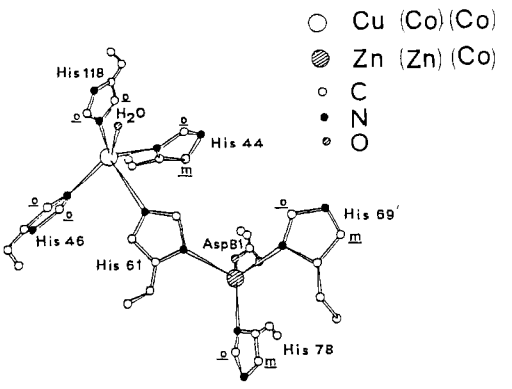


## Experimental Section

Native SOD, purchased from Diagnostic Data Inc. (Mountain View, CA), was used without further purification. Demetalation was obtained as described elsewhere.[8] The $Co_2Zn_2SOD$ derivative was obtained by adding 2 equiv of zinc(II) to the apoprotein at pH 5.9 and then raising the pH to 7.4 and adding 1.4 equiv of cobalt(II) in about 2 days. The $Co_2Co_2SOD$ derivative was obtained by slow addition (2 days) of 3.6 equiv of cobalt(II) to the apoprotein at pH 7.4. Phosphate adducts of the metal-substituted proteins were obtained by titration with phosphate solutions at pH 7.4.

Electronic spectra were run on a Cary 17D spectrophotometer using microcuvettes of 1 cm light path.

Room-temperature 90-MHz $^1H$ NMR spectra were recorded on a Bruker CXP 90 spectrometer, using the modified DEFT sequence[9] described elsewhere[10] with a total recycle time of 0.2 s (8K data points).

(1) Fee, J. A. *J. Biol. Chem.* **1973**, *248*, 4229.
(2) Calabrese, L.; Cocco, D.; Desideri, A. *FEBS Lett.* **1979**, *106*, 142.
(3) Desideri, A.; Cocco, D.; Calabrese, L.; Rotilio, G. *Biochim. Biophys. Acta* **1984**, *785*, 111.
(4) Bertini, I.; Luchinat, C. *Adv. Inorg. Biochem.* **1985**, *6*, 71.
(5) Bertini, I.; Lanini, G.; Luchinat, C.; Messori, L.; Monnanni, R.; Scozzafava, A. *J. Am. Chem. Soc.* **1985**, *107*, 4391.
(6) Bertini, I.; Luchinat, C.; Monnanni, R. *J. Am. Chem. Soc.* **1985**, *107*, 2178.
(7) Bertini, I.; Luchinat, C. *NMR of Paramagnetic Molecules in Biological Systems*; Benjamin Cummings: Boston, 1986.
(8) Pantoliano, M. W.; Valentine, J. S.; Nafie, C. A. *J. Am. Chem. Soc.* **1982**, *104*, 6310.
(9) Hochmann, J.; Kellerhals, H. P. *J. Magn. Reson.* **1980**, *38*, 23.

0020-1669/87/1326-0153$01.50/0 